Journal of Zhejiang University-SCIENCE A (Applied Physics & Engineering)
ISSN 1673-565X (Print); ISSN 1862-1775 (Online)
www.jzus.zju.edu.cn; www.springerlink.com
E-mail: jzus@zju.edu.cn

Stagnation point flow and heat transfer past a permeable stretching/shrinking Riga plate with velocity slip and radiation effects*

Nor Ain Azeany Mohd NASIR[1,2], Anuar ISHAK[2], Ioan POP[†‡3]

[1]*Department of Mathematics, Centre for Defence Foundation Studies, Universiti Pertahanan Nasional Malaysia, Kem Sungai Besi 57000 Kuala Lumpur, Malaysia*

[2]*School of Mathematical Sciences, Faculty of Science and Technology, Universiti Kebangsaan Malaysia, 43600 UKM Bangi, Selangor, Malaysia*

[3]*Department of Mathematics, Babeş-Bolyai University, 400084 Cluj-Napoca, Romania*

[†]E-mail: popm.ioan@yahoo.co.uk

Received Jan. 12, 2018; Revision accepted July 12, 2018; Crosschecked Mar. 11, 2019

Abstract: This paper concerns the stagnation point flow and heat transfer of a viscous and incompressible fluid passing through a flat Riga plate with the effects of velocity slip and radiation. An appropriate similarity transformation is chosen to reduce the governing partial differential equations to a system of ordinary differential equations. The numerical results are verified by comparison with existing results from the literature for a special case of the present study. The computed results are analyzed and given in the form of tables and graphs. The behaviors of the skin friction coefficient and the heat transfer rate for various physical parameters are analyzed and discussed. Dual solutions exist for both stretching and shrinking cases. Stability analysis reveals that the solution with lower boundary layer thickness is stable while the other solution is unstable. It is also observed that for the stable solution, the skin friction coefficient and the local Nusselt number increase as the suction effect is increased. For the shrinking case, a solution exists only for a certain range of the shrinking strength and this range increases with increasing value of the suction effect.

Key words: Riga plate; Stagnation-point flow; Heat transfer; Shrinking sheet; Dual solutions
https://doi.org/10.1631/jzus.A1800029 **CLC number:** O35

1 Introduction

Many researchers have shown interest in studying stagnation point flow because it has many applications such as a jet emerging from slot-jets, melt-spinning processes, glass blowing, and paper production. Hiemenz (1911) was the first to formulate this problem and to solve it numerically. Subsequently, Howarth (1951) extended the problem and considered a steady flow near a cylinder in a moving stream. Years later, Chiam (1994) examined the 2D stagnation point flow through a stretching surface. Recent studies that have dealt with stagnation point flow with varying physical characteristics include Kumari and Nath (1999), Mahapatra and Gupta (2001), Nazar et al. (2004), Yacob and Ishak (2011), and Farooq et al. (2016a), among others. Recently, Bai et al. (2016) explored the magnetohydrodynamic (MHD) Maxwell nanofluid flow near a stagnation point with the thermophoresis effect. They reported

‡ Corresponding author
* Project supported by the Ministry of Education, Malaysia and the Universiti Kebangsaan Malaysia
ORCID: Ioan POP, https://orcid.org/0000-0002-0660-6543

that the computed result of velocity boundary layer thickness is inversely proportional to the stagnation parameter. Another study has been carried out by Hsiao (2016), who considered the stagnation MHD nanofluid mixed convection over a stretching sheet with the effects of a slip boundary. The numerical results revealed that the nano energy conversion produced a higher effect at lower values of the heat sink.

Since the slip velocity was shown to be important in micro devices (Torabi and Peterson, 2016), research has been carried out to explore its impact. One relevant investigation is that on the slip velocity in axially moving micro-concentric cylinders performed by Khadrawi and Al-Shyyab (2010). Assuming that there were no nonlinearities involved, they proposed an analytical solution and stated that the slip velocity at the inner surface is much greater than at the outer surface. Recently, Torabi and Peterson (2016) conducted a study on the impact of slip velocity on entropy generation in microporous channels. Many more studies on the effects of slip velocity have been carried out, for example Chen and Tian (2010), Aziz and Niedbalski (2011), Noghrehabadi et al. (2012), Malvandi and Ganji (2014), and Jha and Aina (2015).

Thermal radiation has an important role in industrial applications such as furnace design, plasma physics, and space craft aerodynamics. There has been much research into the effect of thermal radiation in various problems—for example, those of thermal radiation over a stretching sheet by Cortel (2008) and over a stretching sheet in a nanofluid by Hady et al. (2012). Oyelakin et al. (2016) explored the effect of thermal radiation on an unsteady Casson nanofluid and reported that radiation increases the temperature. Recently, Hsiao (2017a, 2017b, 2017c) investigated the effects of radiation on a stretching sheet in various fluids, while Khan et al. (2017b) studied nonlinear radiation and found that it increases the temperature for all cases considered in the study. Other researchers that have considered nonlinear radiation in their studies include Asadullah et al. (2016), Ahmed et al. (2017a, 2018), and Khan et al. (2017a, 2017c), among others.

However, there has been little research of the characteristics of fluid flows through a Riga plate. A Riga plate is widely known as electromagnetic actuator which comprises a span wise array of permanent magnets and alternating electrodes mounted on a surface (Hayat et al., 2016). It can be used to reduce the skin friction coefficient and pressure drag of a submarine by avoiding boundary layer separation (Farooq et al., 2016b). Among the early researchers who studied this kind of problem are Magyari and Pantokratoras (2011a), who initiated the investigation of the Blasius flow with mixed convection over Riga plates. Then, Hayat et al. (2016) extended the work to a nanofluid flow with variable thickness over a heated Riga plate. In the same year, Farooq et al. (2016b) studied the melting stagnation point flow with homogenous-heterogeneous reaction over variable thickness of a Riga plate. They reported that velocity distribution increased the modified Hartman number. Recently, a number of studies have been carried out on the flow over a Riga plate, such as Ahmad et al. (2016), Ahmed et al. (2017b, 2017c), Ayub et al. (2016), Hayat et al. (2017), and Iqbal et al. (2017).

Although some attention has been given to the flow over a Riga plate, there has been no investigation of the velocity slip and radiation effects of such a flow. Thus, the aim of the present study is to fill that gap. An analysis of stagnation point flow past a permeable stretching/shrinking Riga plate with the effect of velocity slip and radiation is proposed. It is worth mentioning that this work is different from that of Nasir et al. (2017) since they only focused on a quadratically stretching/shrinking surface while this work focusses on the stretching and shrinking Riga plates. The governing equations are reduced from nonlinear partial differential equations to second- and third-order nonlinear ordinary differential equations. The results are computed numerically using the widely used boundary value problem solver, bvp4c, in MATLAB software, together with a shooting technique. The stability of the solutions is analyzed to see the limitation of the bifurcation point and the growth of disturbance in the solutions.

2 Problem formulation

Consider a boundary layer stagnation point flow of a viscous and incompressible fluid past a permeable stretching/shrinking Riga plate with radiation and velocity slip effects as shown in Fig. 1, where x and y

are the Cartesian coordinates measured along the stretching/shrinking surface and normal to it. The flow takes place at $y\geq 0$. It is assumed that both velocities of the stretching/shrinking surface are $u_w(x)$ and that of the ambient (inviscid) fluid is $u_e(x)$. It is also assumed that the constant temperature of the stretching/shrinking surface is T_w, while that of the ambient fluid is T_∞. Further it is assumed that the constant mass velocity is v_0 with $v_0<0$ for suction and $v_0>0$ for injection. Under these conditions, the governing boundary layer equations are (Pantokratoras and Magyari, 2009):

$$\frac{\partial u}{\partial x}+\frac{\partial v}{\partial y}=0, \tag{1}$$

$$\frac{\partial u}{\partial t}+u\frac{\partial u}{\partial x}+v\frac{\partial u}{\partial y} =u_e\frac{\mathrm{d}u_e}{\mathrm{d}x}+\nu\frac{\partial^2 u}{\partial y^2}+\frac{\pi j_0 M_0}{8\rho}\exp\left(-\frac{\pi}{\alpha_1}y\right), \tag{2}$$

$$\frac{\partial T}{\partial t}+u\frac{\partial T}{\partial x}+v\frac{\partial T}{\partial y} =\alpha\frac{\partial^2 T}{\partial y^2}+\frac{16\sigma^* T_\infty^3}{3k^*\rho C_p}\frac{\partial^2 T}{\partial y^2}, \tag{3}$$

along with the initial and boundary conditions:

$$\left.\begin{aligned} &u=u_w(x)=\lambda U_w(x)+N\frac{\partial u}{\partial y},\\ &v=v_0,\quad T=T_w,\end{aligned}\right\}\text{at}\quad y=0,\\ u\to u_e(x)=ax,\quad T\to T_\infty\quad\text{as}\quad y\to\infty, \tag{4}$$

where u and v are the velocity components along the x and y axes, respectively, t is the time, λ is the constant stretching/shrinking parameter with $\lambda>0$ corresponding to the stretching and $\lambda<0$ to the shrinking sheet, and we assume that $U_w(x)=ax$, where a is a positive constant. Further, α is the thermal diffusivity, ν is the kinematic viscosity, ρ denotes the density, j_0 represents the applied current density in the electrodes, M_0 represents the magnetization of the permanent magnets, α_1 is the width for electrodes and magnets, σ^* denotes the Stefan-Boltzman constant, C_p is the specific heat at constant pressure, k^* denotes the mean absorption coefficient, and N is the velocity slip coefficient. We notice that the last term in Eq. (3) is the radiation term based on the Roseland approximation (Magyari and Pantokratoras, 2011b).

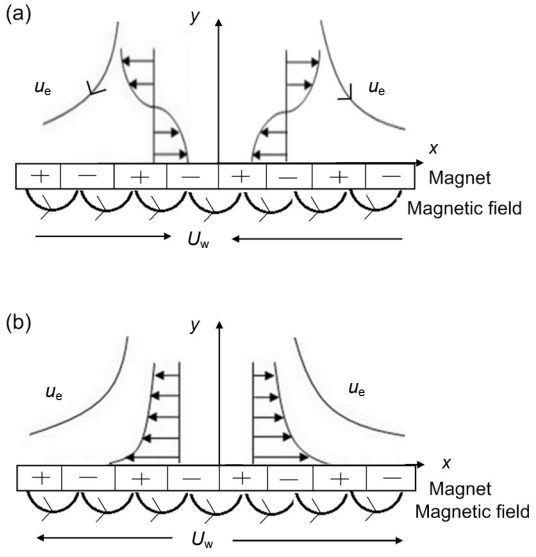

Fig. 1 Physical model of a Riga plate with shrinking sheet (a) and stretching sheet (b)

3 Solution for the steady problem

In order to solve Eqs. (1)–(3) subject to the boundary conditions Eq. (4), we assume that $M_0=x\tilde{M}_0$, where $\tilde{M}_0$ is the characteristic magnetization of the permanent magnets. Thus, we introduce the following similarity variables (Kuznetsov and Nield, 2010):

$$u=axf'(\eta),\quad v=-\sqrt{a\alpha}f(\eta),\\ \theta(\eta)=\frac{T-T_\infty}{T_w-T_\infty},\quad \eta=\sqrt{a/\alpha}y, \tag{5}$$

where primes denote differentiation with respect to η, f is the dimensionless stream function and θ is the dimensionless temperature. Substituting the variables Eq. (5) into Eqs. (1)–(3), it is found that the continuity equation Eq. (1) is automatically satisfied, and Eqs. (2) and (3) are reduced to the following ordinary (similarity) differential equations:

$$Prf'''+ff''+1-f'^2+Q\mathrm{e}^{-\eta}=0, \tag{6}$$

$$\left(1+\frac{4}{3}\mathrm{Rd}\right)\theta''+f\theta'=0, \tag{7}$$

subject to the boundary conditions:

$$\begin{aligned} &f(0)=S, \quad f'(0)=\lambda+\beta f''(0), \quad \theta(0)=1,\\ &f'(\eta)\to 1, \quad \theta(\eta)\to 0 \quad \text{as} \quad \eta\to\infty. \end{aligned} \tag{8}$$

Here S is the surface mass transfer parameter with $S>0$ for suction, $S<0$ for injection, and $S=0$ for the impermeable plate. Pr is the Prandtl number, Rd is the radiation parameter, Q is the modified Hartman number, and β is the velocity slip parameter, which are defined as

$$\begin{aligned} &S=-\frac{v_0}{\sqrt{a\alpha}}, \quad Pr=\frac{\nu}{\alpha}, \quad \mathrm{Rd}=\frac{4\sigma^* T_\infty^3}{kk^*},\\ &Q=\frac{\pi j_0 \tilde{M}_0}{8a^2\rho}, \quad \beta=N\sqrt{a/\alpha}. \end{aligned} \tag{9}$$

It should be stressed that the use of the variables in Eq. (5) moves the Prandtl number from the energy equation Eq. (7) to the momentum equation Eq. (6). That is a new fact for stretching/shrinking sheet problems.

The physical quantities of practical interest are the skin friction or shear stress coefficient C_f and the local Nusselt number Nu_x, which are defined as

$$C_\mathrm{f}=\frac{\tau_\mathrm{w}}{\rho U_\mathrm{w}^2}, \quad Nu_x=\frac{xq_\mathrm{w}}{k(T_\mathrm{w}-T_\infty)}, \tag{10}$$

where τ_w is the skin friction or the shear stresses, and q_w is the heat flux from the surface of the sheet, which are given by

$$\begin{aligned} &\tau_\mathrm{w}=\mu\left(\frac{\partial u}{\partial y}\right)_{y=0},\\ &q_\mathrm{w}=-k\left(1+\frac{4}{3}\mathrm{Rd}\right)\left(\frac{\partial T}{\partial y}\right)_{y=0}, \end{aligned} \tag{11}$$

where μ is the dynamic viscosity

Substituting Eq. (5) into Eq. (10) and using Eq. (11), we can obtain:

$$\begin{aligned} &Re_x^{1/2}\,C_\mathrm{f}=f''(0),\\ &Re_x^{-1/2}\,Nu_x=\left(1+\frac{4}{3}\mathrm{Rd}\right)\left[-\theta'(0)\right], \end{aligned} \tag{12}$$

where $Re_x=u_\mathrm{e}(x)x/\alpha$ is the local Reynolds number.

4 Flow stability

In order to perform the stability analysis, a dimensionless similarity transformation is introduced as follows:

$$\begin{aligned} &U=aX\frac{\partial F}{\partial \eta}(\eta,\tau), \quad V=-\sqrt{a\alpha}F(\eta,\tau),\\ &\theta(\eta,\tau)=\frac{T-T_\infty}{T_\mathrm{w}-T_\infty}, \quad \eta=\sqrt{a/\alpha}\,Y, \quad \tau=at. \end{aligned} \tag{13}$$

Hence, the unsteady equations Eqs. (2) and (3) respectively reduce to:

$$Pr\frac{\partial^3 f}{\partial\eta^3}+f\frac{\partial^2 f}{\partial\eta^2}+1-\left(\frac{\partial f}{\partial\eta}\right)^2+Q\mathrm{e}^{-\eta}-\frac{\partial^2 f}{\partial\eta\partial\tau}=0, \tag{14}$$

$$\left(1+\frac{4}{3}\mathrm{Rd}\right)\frac{\partial^2\theta}{\partial\eta^2}+f\frac{\partial\theta}{\partial\eta}-\frac{\partial\theta}{\partial\tau}=0, \tag{15}$$

with boundary conditions:

$$\begin{aligned} &f(0,\tau)=S, \quad \frac{\partial f}{\partial\eta}(0,\tau)=\lambda+\beta\frac{\partial^2 f}{\partial\eta^2}(0,\tau),\\ &\theta(0,\tau)=1,\\ &\frac{\partial f}{\partial\eta}(\eta,\tau)\to 1, \quad \theta(\eta,\tau)\to 0 \quad \text{as} \quad \eta\to\infty. \end{aligned} \tag{16}$$

Following Weidman et al. (2006) and Rosca and Pop (2013), we employ basic equations with disturbances given by

$$\begin{aligned} &f(\eta,\tau)=f_0(\eta)+\mathrm{e}^{-\gamma\tau}F(\eta),\\ &\theta(\eta,\tau)=h_0(\eta)+\mathrm{e}^{-\gamma\tau}H(\eta), \end{aligned} \tag{17}$$

where γ is an unknown eigenvalue and $F(\eta)$ and $H(\eta)$ are small relative to $f_0(\eta)$ and $h_0(\eta)$ (Awaludin et al., 2016). Substituting Eq. (17) into the transformed unsteady equations Eqs. (14) and (15) gives:

$$PrF'''+f_0F''+\left(\gamma-2f_0'\right)F'+f_0''F=0, \tag{18}$$

$$\left(1+\frac{4}{3}\mathrm{Rd}\right)H''+f_0H'+h_0'F'+\gamma H=0, \tag{19}$$

subject to the boundary conditions:

$$F(0)=0,\quad F'(0)=\beta F''(0),\quad H(0)=0,\\ F'(\eta)\to 0,\quad H(\eta)\to 0\quad \text{as}\quad \eta\to\infty. \tag{20}$$

It is worth mentioning that, based on Eq. (17), if the smallest eigenvalue γ is negative then there is a growth of disturbance as time τ increases and thus the flow will become unstable. In contrast, if the smallest eigenvalue γ is positive, there is a decay of disturbance as time passes, and the flow is said to be stable.

5 Results and discussion

The objective of this section is to uncover the behaviors of the skin friction coefficient, local Nusselt number, velocity profiles, and temperature profiles corresponding to a variety of physical parameters. The nonlinear ordinary differential equations Eqs. (6) and (7) subjected to the boundary conditions Eq. (8) were solved numerically using a built-in boundary value problem solver in MATLAB software, namely bvp4c. The relative tolerance is set to 10^{-10} to ensure the accuracy of the numerical results and the finite value of $\eta\to\infty$ is chosen to be η=15 to establish the converging of the numerical results obtained later. Tables 1 and 2 show the comparisons of the numerical results with the earlier published results by Rosca et al. (2016), Abd El-Aziz (2016), and Nandy and Pop (2014) for validation purposes. As we can clearly see that all results are in good agreement and thus the present numerical results are validated.

Fig. 2 is plotted to see the relationship between the stretching/shrinking parameter λ and the skin friction coefficient $Re_x^{1/2}C_f$ when the suction strength S is increased. As we can see, when S is increased, the solution domain for λ also increases. The minimum values of λ for which the solution exists for S=0, 2.5, 3.0, 3.5 are λ_c=−1.699, −6.976, −9.361, −11.780, respectively. It is also noticeable that the second solution (lower branch solution) existed for $\lambda_c<\lambda<0$ (shrinking case) and $\lambda\geq 0$ (stretching case). This figure also emphasizes that the range of $Re_x^{1/2}C_f$ increases as the value of the suction strength increases. Additionally, when λ=1, $Re_x^{1/2}C_f$=0, due to the fluid and the boundary moving with the same velocity and thus not producing any friction at the fluid-solid interface (Sharma et al., 2014).

The variations of the local Nusselt number $Re_x^{-1/2}Nu_x$ for suction strengths S=0, 2.5, 3.0, 3.5 are

Table 1 Comparison of $f''(0)$ for S=Q=Rd=0, Pr=1.0, and λ<0 (shrinking sheet)

λ	$f''(0)$					
	Present study		Rosca et al. (2016)		Abd El-Aziz (2016)	
	Upper branch	Lower branch	Upper branch	Lower branch	Upper branch	Lower branch
−0.2500	1.4022408	–	1.402240	–	1.4022408	–
−0.5000	1.4956697	–	1.495669	–	1.4956698	–
−0.7500	1.4892982	–	1.489298	–	1.4892983	–
−1.0000	1.3288168	0.000000	1.328816	0.000000	1.3288169	0.0000000
−1.1000	1.1866802	0.049229	1.186680	0.049228	1.1866804	0.0492289
−1.1500	1.0822311	0.116702	1.082231	0.116702	1.0822314	0.1167021
−1.2000	0.9324733	0.233650	0.932473	0.233649	0.9324740	0.2336497
−1.2465	0.5842816	0.554296	0.584281	0.554292	0.5842915	0.5542856

Table 2 Comparison of $f''(0)$ for S=Q=Rd=0, Pr=1.0, and λ>0 (stretching sheet)

λ	$f''(0)$		
	Present study	Rosca et al. (2016)	Nandy and Pop (2014)
0.0	1.23258800	1.232587	1.232588
0.2	1.05113000	1.051129	1.051131
0.5	0.71329500	0.713294	0.713296
1.0	0.00000000	0.000000	0.000000
2.0	−1.88730700	−1.887306	−1.887307
5.0	−10.2647490	−10.264749	−10.264751
8.0	−21.6847996	–	–

shown in Fig. 3. Fig. 3 shows the same pattern as Fig. 2. The values of $Re_x^{-1/2}Nu_x$ which represent the heat transfer rates at the surface increase as the strength of suction increases. This happens because suction increases the friction at the fluid-solid interface and, in consequence, increases the local Nusselt number $Re_x^{-1/2}Nu_x$. It is also demonstrated that the domain for λ increases and the values for critical λ_c decrease as the strength of suction increases. It is the same as in Fig. 2 where dual solutions exist for both shrinking and stretching cases.

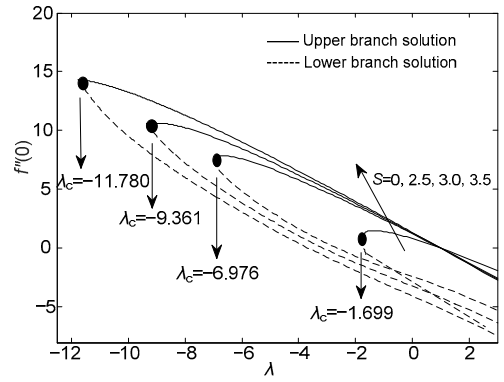

Fig. 2 Variation of skin friction coefficient $f''(0)$ when suction, S=0, 2.5, 3.0, 3.5 with Q=0.6, β=0.5, Pr=1.0

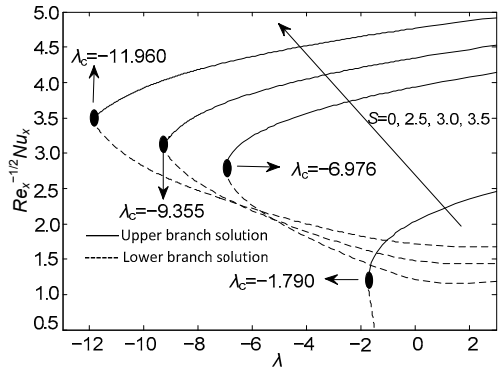

Fig. 3 Variation of local Nusselt number $Re_x^{1/2}Nu_x$ when suction, S=0, 2.5, 3.0, 3.5 with Q=0.6, Rd=0.5, β=0.5, Pr=1.0

Fig. 4 shows the variation of the skin friction coefficient $Re_x^{1/2}C_f$ with S for the shrinking case (λ=−2.0, −2.5, −3.0). It is clear that as λ increases, the domain of S increases. The critical values of S when λ=−2.0, −2.5, −3.0 are S_c=0.2998, 0.6535, 0.9792, respectively. The value of $Re_x^{1/2}C_f$ decreases as λ increases. Moreover, its range increases as suction S increases. When S_c=0.9792, 0.6535, 0.2998, the values of $Re_x^{1/2}C_f$ are 2.608, 2.041, 1.545, respectively. Dual solutions exist for all values of $S>S_c$, while there is no solution when $S<S_c$.

The graph of $Re_x^{-1/2}Nu_x$ is plotted for different values of λ as shown in Fig. 5. The local Nusselt number $Re_x^{-1/2}Nu_x$ increases as λ decreases. It is observed that the domain for S decreases as the value of λ decreases. It is also observed that the range of $Re_x^{-1/2}Nu_x$ decreases as the critical values of S increase. The second solution (lower branch solution) exists when $S>S_c$. It is shown that the values of $Re_x^{-1/2}Nu_x$ when S_c=0.2998, 0.6535, 0.9831 are $Re_x^{-1/2}Nu_x$=1.448, 1.646, 1.8605, respectively.

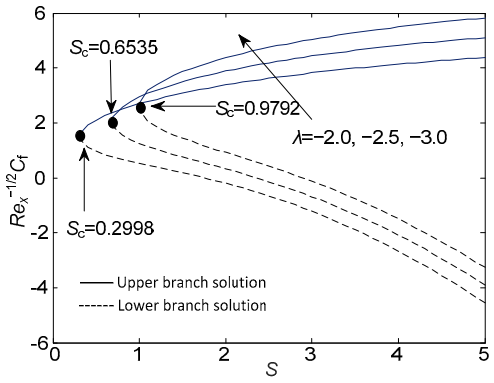

Fig. 4 Variation of $Re_x^{1/2}C_f$ when λ=−2.0, −2.5, −3.0 with Q=0.6, β=0.5, Pr=1.0

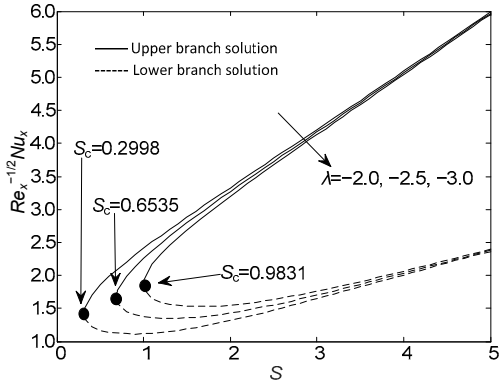

Fig. 5 Variation of $Re_x^{-1/2}Nu_x$ when λ=−2.0, −2.5, −3.0 with Q=0.6, Rd=0.5, β=0.5, Pr=1.0

The effect of the radiation parameter Rd on the temperature profiles, $\theta(\eta)$ is illustrated in Fig. 6. It can be seen that the temperature distribution increases as the value of Rd increases. In addition, the thermal boundary layer thickness is enhanced for increased

values of the thermal radiation, Rd. This is due to the inter-atomic collisions which can cause the increase of the kinetic energy of the fluid molecule to change and thus will enhance the temperature distribution of the fluid.

The effects of slip velocity β on the velocity and the temperature can be seen in Figs. 7 and 8. Fig. 7 shows the influence of β towards the velocity profiles, $f'(\eta)$. It is clearly seen that the slip velocity β, enhances the velocity as β moves to higher values. This can be explained by Stoke's law which is related to the fluid density. Increasing the density of the fluid will result in an increase in the slip velocity and thus will increase the velocity difference between the fluid and the plate. Fig. 8 shows the impact of the slip parameter β on the temperature profiles $\theta(\eta)$. The temperature decreases as the slip strength increases. This is because the viscosity of the fluid tends to increase as its temperature decreases.

It is noticeable from Figs. 2 and 3 that dual solutions exist for both stretching and shrinking cases. A stability analysis is carried out to determine which of the solutions is stable and which is not. We solve the eigenvalue problem Eqs. (18)–(20), and find the smallest values γ in Eq. (17). Positive values of γ show that there is an initial decay of disturbance as time passes, $\tau\to\infty$. In contrast, negative values of γ indicate initial growth of disturbance, and thus cause the instability of the flow. In Fig. 9, it is clearly shown that the positive values of γ (which represent the upper branch solution) show it is stable while the lower branch solution, which is represented by negative values of γ, is unstable. The change of sign of γ from positive to negative occurs at the bifurcation point $\lambda=\lambda_c$.

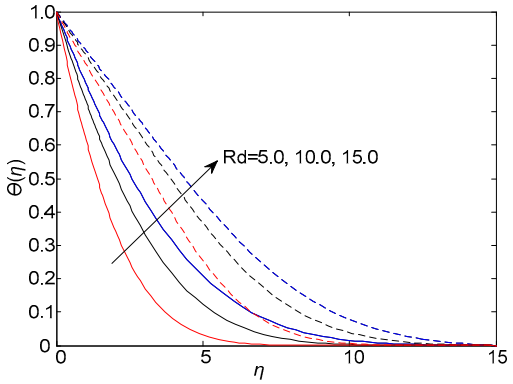

Fig. 6 Effect of Rd on temperature profile $\theta(\eta)$ with Q=0.6, λ=−2.0, β=0.5, η=15.0, Pr=1.0, S=2.0

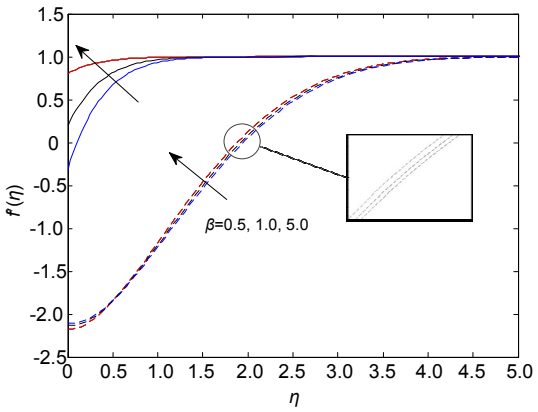

Fig. 7 Effect of β on velocity profile $f'(\eta)$ with Q=0.6, Rd=5.0, λ=−2.0, η=15.0, Pr=1.0, S=2.0

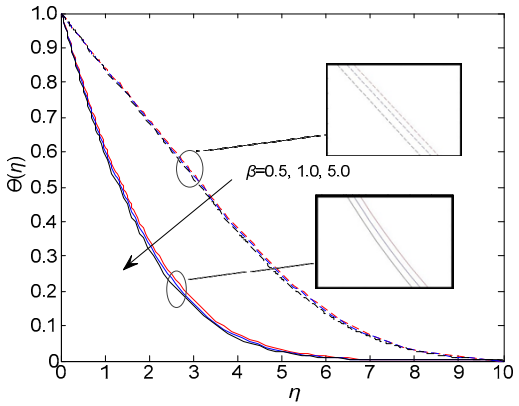

Fig. 8 Effect of β on temperature profile $\theta(\eta)$ with Q=0.6, Rd=5.0, λ=−2.0, Pr=1.0, S=2.0

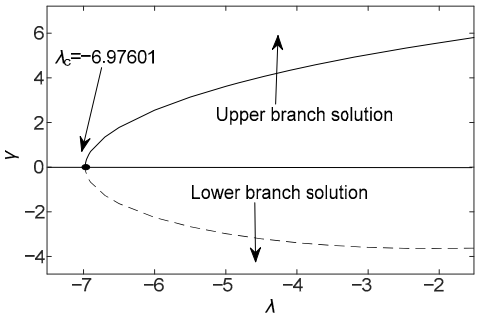

Fig. 9 The smallest eigenvalues γ for selected values of λ with Pr=1.0, β=0.5, Rd=5.0

6 Conclusions

The characteristics of a stretching/shrinking Riga plate have been analyzed with reference to the effects of velocity slip and radiation. Dual solutions have been found for both stretching and shrinking cases. A stability analysis has been carried out to deal

with the dual solutions, and this determined which of the solutions is stable. It was found that the upper branch solution is stable and the lower branch solution is not. The numerical results can be summarized as follows:

1. The skin friction coefficient and the heat transfer rate increase as the strength of suction is increased.

2. The skin friction coefficient decreases as the stretching/shrinking parameter λ increases, for both solution branches.

3. The local Nusselt number which represents the heat transfer rate at the surface increases for the upper solution branch but decreases for the lower branch.

4. A higher value of radiation will result in an enhanced temperature.

5. Increasing the slip effect will enhance the velocity but decrease the temperature inside the boundary layer.

References

Abd El-Aziz M, 2016. Dual solutions in hydromagnetic stagnation point flow and heat transfer towards a stretching/shrinking sheet with non-uniform heat source/sink and variable surface heat flux. *Journal of the Egyptian Mathematical Society*, 24(3):479-486. https://doi.org/10.1016/j.joems.2015.09.004

Ahmad A, Asghar S, Afzal S, 2016. Flow of nanofluid past a Riga plate. *Journal of Magnetism and Magnetic Materials*, 402:44-48. https://doi.org/10.1016/j.jmmm.2015.11.043

Ahmed N, Khan U, Mohyud-Din ST, 2017a. Influence of nonlinear thermal radiation on the viscous flow through a deformable asymmetric porous channel: a numerical study. *Journal of Molecular Liquids*, 225:167-173.

Ahmed N, Khan U, Mohyud-Din ST, 2017b. Influence of thermal radiation and viscous dissipation on squeezed flow of water between Riga plates saturated with carbon nanotubes. *Colloids and Surfaces A*: *Physicochemical and Engineering Aspects*, 522:389-398. https://doi.org/10.1016/j.colsurfa.2017.02.083

Ahmed N, Khan U, Mohyud-Din ST, et al., 2017c. Shape effects of nanoparticles on the Squeezed flow between two Riga Plates in the presence of thermal radiation. *The European Physical Journal Plus*, 132(7):321. https://doi.org/10.1140/epjp/i2017-11576-7 https://doi.org/10.1016/j.molliq.2016.11.021

Ahmed N, Khan U, Mohyud-Din ST, et al., 2018. A finite element investigation of the flow of a Newtonian fluid in dilating and squeezing porous channel under the influence of nonlinear thermal radiation. *Neural Computing and Applications*, 29(2):501-508. https://doi.org/10.1007/s00521-016-2463-9

Asadullah M, Khan U, Ahmed N, et al., 2016. Analytical and numerical investigation of thermal radiation effects on flow of viscous incompressible fluid with stretchable convergent/divergent channels. *Journal of Molecular Liquids*, 224:768-775. https://doi.org/10.1016/j.molliq.2016.10.073

Awaludin IS, Weidman PD, Ishak A, 2016. Stability analysis of stagnation-point flow over a stretching/shrinking sheet. *AIP Advances*, 6(4):045308. https://doi.org/10.1063/1.4947130

Ayub M, Abbas T, Bhatti MM, 2016. Inspiration of slip effects on electromagnetohydrodynamics (EMHD) nanofluid flow through a horizontal Riga plate. *The European Physical Journal Plus*, 131(6):193. https://doi.org/10.1140/epjp/i2016-16193-4

Aziz A, Niedbalski N, 2011. Thermally developing microtube gas flow with axial conduction and viscous dissipation. *International Journal of Thermal Sciences*, 50(3):332-340. https://doi.org/10.1016/j.ijthermalsci.2010.08.003

Bai Y, Liu XL, Zhang Y, et al., 2016. Stagnation-point heat and mass transfer of MHD Maxwell nanofluids over a stretching surface in the presence of thermophoresis. *Journal of Molecular Liquids*, 224:1172-1180. https://doi.org/10.1016/j.molliq.2016.10.082

Chen S, Tian ZW, 2010. Simulation of thermal micro-flow using lattice Boltzmann method with Langmuir slip model. *International Journal of Heat and Fluid Flow*, 31(2):227-235. https://doi.org/10.1016/j.ijheatfluidflow.2009.12.006

Chiam TC, 1994. Stagnation-point flow towards a stretching plate. *Journal of the Physical Society of Japan*, 63(6):2443-2444. https://doi.org/10.1143/JPSJ.63.2443

Cortel R, 2008. Effects of viscous dissipation and radiation on the thermal boundary layer over a nonlinearly stretching sheet. *Physics Letters A*, 372(5):631-636. https://doi.org/10.1016/j.physleta.2007.08.005

Farooq M, Khan MI, Waqas M, et al., 2016a. MHD stagnation point flow of viscoelastic nanofluid with non-linear radiation effects. *Journal of Molecular Liquids*, 221:1097-1103. https://doi.org/10.1016/j.molliq.2016.06.077

Farooq M, Anjum A, Hayat T, et al., 2016b. Melting heat transfer in the flow over a variable thicked Riga plate with homogeneous-heterogeneous reactions. *Journal of Molecular Liquids*, 224:1341-1347. https://doi.org/10.1016/j.molliq.2016.10.123

Hady FM, Ibrahim FS, Abdel-Gaied SM, et al., 2012. Radiation effect on viscous flow of a nanofluid and heat transfer over a nonlinearly stretching sheet. *Nanoscale Research Letters*, 7(1):229. https://doi.org/10.1186/1556-276X-7-229

Hayat T, Abbas T, Ayub M, et al., 2016. Flow of nanofluid due to convectively heated Riga plate with variable thickness.

Journal of Molecular Liquids, 222:854-862. https://doi.org/10.1016/j.molliq.2016.07.111

Hayat T, Khan M, Imtiaz M, et al., 2017. Squeezing flow past a Riga plate with chemical reaction and convective conditions. *Journal of Molecular Liquids*, 225:569-576. https://doi.org/10.1016/j.molliq.2016.11.089

Hiemenz K, 1911. Die Grenzschicht an einem in den gleichformingen Flussigkeitsstrom einge-tauchten graden Kreiszylinder. *Dingler's Polytechnisches Journal*, 326: 321-324 (in German).

Howarth L, 1951. The boundary layer in three dimensional flow. Part II. The flow near a stagnation point. *Philosophical Magazine*, 42(7):1433-1440.

Hsiao KL, 2016. Stagnation electrical MHD nanofluid mixed convection with slip boundary on a stretching sheet. *Applied Thermal Engineering*, 98:850-861. https://doi.org/10.1016/j.applthermaleng.2015.12.138

Hsiao KL, 2017a. Combined electrical MHD heat transfer thermal extrusion system using Maxwell fluid with radiative and viscous dissipation effects. *Applied Thermal Engineering*, 112:1281-1288. https://doi.org/10.1016/j.applthermaleng.2016.08.208

Hsiao KL, 2017b. Micropolar nanofluid flow with MHD and viscous dissipation effects towards a stretching sheet with multimedia feature. *International Journal of Heat and Mass Transfer*, 112:983-990. https://doi.org/10.1016/j.ijheatmasstransfer.2017.05.042

Hsiao KL, 2017c. To promote radiation electrical MHD activation energy thermal extrusion manufacturing system efficiency by using Carreau-nanofluid with parameters control method. *Energy*, 130:486-499. https://doi.org/10.1016/j.energy.2017.05.004

Iqbal Z, Mehmood Z, Azhar E, et al., 2017. Numerical investigation of nanofluidic transport of gyrotactic microorganisms submerged in water towards Riga plate. *Journal of Molecular Liquids*, 234:296-308. https://doi.org/10.1016/j.molliq.2017.03.074

Jha BK, Aina B, 2015. Mathematical modelling and exact solution of steady fully developed mixed convection flow in a vertical micro-porous-annulus. *Afrika Matematika*, 26(7-8):1199-1213. https://doi.org/10.1007/s13370-014-0277-4

Khadrawi AF, Al-Shyyab A, 2010. Slip flow and heat transfer in axially moving micro-concentric cylinders. *International Communications in Heat and Mass Transfer*, 37(8):1149-1152. https://doi.org/10.1016/j.icheatmasstransfer.2010.06.006

Khan U, Ahmed N, Bin-Mohsen B, et al., 2017a. Nonlinear radiation effects on flow of nanofluid over a porous wedge in the presence of magnetic field. *International Journal of Numerical Methods for Heat & Fluid Flow*, 27(1):48-63. https://doi.org/10.1108/HFF-10-2015-0433

Khan U, Ahmed N, Mohyud-Din ST, et al., 2017b. Nonlinear radiation effects on MHD flow of nanofluid over a nonlinearly stretching/shrinking wedge. *Neural Computing and Applications*, 28(8):2041-2050. https://doi.org/10.1007/s00521-016-2187-x

Khan U, Abbasi A, Ahmed N, et al., 2017c. Particle shape, thermal radiations, viscous dissipation and joule heating effects on flow of magneto-nanofluid in a rotating system. *Engineering Computations*, 34(8):2479-2498. https://doi.org/10.1108/EC-04-2017-0149

Kumari M, Nath G, 1999. Development of flow and heat transfer of a viscous fluid in the stagnation-point region of a three-dimensional body with a magnetic field. *Acta Mechanica*, 135(1-2):1-12. https://doi.org/10.1007/BF01179042

Kuznetsov AV, Nield DA, 2010. Natural convective boundary-layer flow of a nanofluid past a vertical plate. *International Journal of Thermal Sciences*, 49(2):243-247. https://doi.org/10.1016/j.ijthermalsci.2009.07.015

Magyari E, Pantokratoras A, 2011a. Aiding and opposing mixed convection flows over the Riga-plate. *Communications in Nonlinear Science and Numerical Simulation*, 16(8):3158-3167. https://doi.org/10.1016/j.cnsns.2010.12.003

Magyari E, Pantokratoras A, 2011b. Note on the effect of thermal radiation in the linearized Rosseland approximation on the heat transfer characteristics of various boundary layer flows. *International Communications in Heat and Mass Transfer*, 38(5):554-556. https://doi.org/10.1016/j.icheatmasstransfer.2011.03.006

Mahapatra TR, Gupta AS, 2001. Magnetohydrodynamic stagnation-point flow towards a stretching sheet. *Acta Mechanica*, 152(1-4):191-196. https://doi.org/10.1007/BF01176953

Malvandi A, Ganji DD, 2014. Mixed convective heat transfer of water/alumina nanofluid inside a vertical microchannel. *Powder Technology*, 263:37-44. https://doi.org/10.1016/j.powtec.2014.04.084

Nandy SK, Pop I, 2014. Effects of magnetic field and thermal radiation on stagnation flow and heat transfer of nanofluid over a shrinking surface. *International Communications in Heat and Mass Transfer*, 53:50-55. https://doi.org/10.1016/j.icheatmasstransfer.2014.02.010

Nasir NAAM, Ishak A, Pop I, 2017. Stagnation-point flow and heat transfer past a permeable quadratically stretching/shrinking sheet. *Chinese Journal of Physics*, 55(5): 2081-2091. https://doi.org/10.1016/j.cjph.2017.08.023

Nazar R, Amin N, Filip D, et al., 2004. Unsteady boundary layer flow in the region of the stagnation point on a stretching sheet. *International Journal of Engineering Science*, 42(11-12):1241-1253. https://doi.org/10.1016/j.ijengsci.2003.12.002

Noghrehabadi A, Pourrajab R, Ghalambaz M, 2012. Effect of partial slip boundary condition on the flow and heat transfer of nanofluids past stretching sheet prescribed constant wall temperature. *International Journal of Thermal Sciences*, 54:253-261. https://doi.org/10.1016/j.ijthermalsci.2011.11.017

Oyelakin IS, Mondal S, Sibanda P, 2016. Unsteady Casson nanofluid flow over a stretching sheet with thermal radiation, convective and slip boundary conditions. *Alexandria Engineering Journal*, 55(2):1025-1035. https://doi.org/10.1016/j.aej.2016.03.003

Pantokratoras A, Magyari E, 2009. EMHD free-convection boundary-layer flow from a Riga-plate. *Journal of Engineering Mathematics*, 64(3):303-315. https://doi.org/10.1007/s10665-008-9259-6

Rosca AV, Rosca NC, Pop I, 2016. Numerical simulation of the stagnation point flow past a permeable stretching/shrinking sheet with convective boundary condition and heat generation. *International Journal of Numerical Methods for Heat & Fluid Flow*, 26(1):348-364. https://doi.org/10.1108/HFF-12-2014-0361

Rosca NC, Pop I, 2013. Mixed convection stagnation point flow past a vertical flat plate with a second order slip: heat flux case. *International Journal of Heat and Mass Transfer*, 65:102-109. https://doi.org/10.1016/j.ijheatmasstransfer.2013.05.061

Sharma R, Ishak A, Pop I, 2014. Stability analysis of magnetohydrodynamic stagnation-point flow toward a stretching/shrinking sheet. *Computers & Fluids*, 102:94-98. https://doi.org/10.1016/j.compfluid.2014.06.022

Torabi M, Peterson GP, 2016. Effects of velocity slip and temperature jump on the heat transfer and entropy generation in micro porous channels under magnetic field. *International Journal of Heat and Mass Transfer*, 102:585-595. https://doi.org/10.1016/j.ijheatmasstransfer.2016.06.080

Weidman PD, Kubitschek DG, Davis AMJ, 2006. The effect of transpiration on self-similar boundary layer flow over moving surfaces. *International Journal of Engineering Science*, 44(11-12):730-737. https://doi.org/10.1016/j.ijengsci.2006.04.005

Yacob NA, Ishak A, 2011. MHD flow of a micropolar fluid towards a vertical permeable plate with prescribed surface heat flux. *Chemical Engineering Research and Design*, 89(11):2291-2297. https://doi.org/10.1016/j.cherd.2011.03.011

中文概要

题　目：通过具有速度滑移和辐射效应的可渗透拉伸/收缩 Riga 板的驻点流动和热传导

目　的：1. 通过分析 Riga 板的抽吸效应来控制流体运动和减少摩擦力和压力阻力；2. 利用磁场的速度滑移效应来控制流体的流速；3. 基于辐射原理控制热传导并减小阻力。

创新点：1. 本研究可应用于核电厂、飞机、潜艇以及卫星等设施中推进装置的设计；2. 本研究可用于防止边界层分离以减少湍流的产生。

方　法：1. 构建基于偏微分方程的数理模型；2. 利用相似变换法将偏微分方程简化为常微分方程；3. 利用 Matlab 内置求解器 bvp4c 对常微分方程组进行数值求解；4. 基于求解结果讨论稳定性。

结　论：1. 对于拉伸/收缩两种情形的 Riga 板问题都存在对偶解；2. 数值求解结果显示表面摩擦系数和表面传热率均会随着吸力的增大而增大，而随拉伸/收缩参数λ的增大而减小；3. 上支解的努塞尔数增大而下支解减小；4. 辐射会提高边界层内的温度，而增强滑移效应则会提高流速同时降低边界层温度；5. 只有上支解是长期稳定的。

关键词：Riga 板；驻点流动；热传导；收缩薄片；对偶解